

Stability of anisotropic superconducting phases in UPt₃

W. Putikka and Robert Joynt

Physics Department, 1150 University Avenue, University of Wisconsin-Madison, Madison, Wisconsin 53706

(Received 26 October 1987)

We have calculated the relative stability of *s*-, *p*-, and *d*-wave superconducting states in UPt₃. This is done by fitting the observed spin-fluctuation spectrum by a simple form and taking the exchange of these fluctuations as the pairing mechanism. One representative of each of the above classes of states can occur, the stability depending on the Coulomb pseudopotential, the details of the fluctuation spectrum, and the Fermi surface. The most favorable gap function for the *d*-wave representations has two lines of nodes.

Much of the excitement surrounding the discovery of heavy-fermion systems has been due to the fact that they exhibit anisotropic superconducting phases. This has led to controversy surrounding the nature of the phases, and the superconductivity mechanism.¹

The exchange of spin fluctuations as a means of pairing in heavy-fermion superconductors has been considered by several authors.²⁻⁹ From calculations on ³He it is known that ferromagnetic spin fluctuations suppress conventional singlet pairing and lead to triplet pairing.¹⁰⁻¹⁴ The spin fluctuations observed by neutron scattering¹⁵ in UPt₃ are antiferromagnetic, tending toward an ordering wave vector $\mathbf{q} = (2\pi/c)\hat{z}$. Previous work on antiferromagnetic spin fluctuations⁵⁻⁹ has led to the conclusion that they suppress both conventional singlet and triplet pairing,⁶⁻⁸ but they promote anisotropic singlet pairing.^{5,7,9}

Our purpose in this Rapid Communication is to examine this reasoning in a phenomenological spirit for UPt₃. Enough is now known about the spin-fluctuation spectrum from neutron scattering¹⁵ and about the Fermi surface from calculations¹⁶⁻¹⁸ and de Haas-van Alphen experiments¹⁹ that serious calculations of the relative stability of different superconducting phases can be carried out. Our treatment differs from an earlier paper⁹ along these lines by incorporating the group-theoretical analysis of the possible phases and by demanding that the electronic wave function be completely antisymmetric. We follow this paper in neglecting spin-orbit coupling, with consequences to be noted below.

The model we consider is that of Anderson and Brinkman¹¹ and Nakajima.¹² The effective interaction Hamil-

tonian is

$$H_{int} = \frac{1}{2} \sum_{kk'} \sum_q \frac{3}{4} I^2 \chi(k-k') \sigma_{\alpha\beta} \cdot \sigma_{\gamma\delta} a_{k+q/2,\alpha}^\dagger a_{-k+q/2,\gamma}^\dagger \times a_{-k'+q/2,\delta} a_{k'+q/2,\beta}, \tag{1}$$

where $\chi(\mathbf{q})$, the static susceptibility, is a phenomenological function determined from the neutron scattering data and *I* is the Hubbard interaction parameter.

The \mathbf{q} dependence of $\chi(\mathbf{q})$ is found from the neutron scattering data of Aeppli *et al.*¹⁵ Along the *z* axis the data are fitted to within experimental error by

$$\chi(q_z) = \chi_a - \chi_b \cos\left(\frac{q_z c}{2}\right), \tag{2}$$

where χ_a, χ_b are positive constants and $\chi_a/\chi_b = 3.44$. Note that the parabolic forms of $\chi(q_z)$ chosen in Ref. 9 are not consistent with the data at large *q*. The q_x and q_y dependence has not been fully mapped out experimentally and must be determined in a more indirect fashion. The short-range antiferromagnetic spin fluctuations in UPt₃ are consistent with the spins in a single basal plane tending to be parallel and spins in neighboring planes displaced by *c*/2 tending to be antiparallel.¹⁵

These observations lead us to take the simple form $\chi(\mathbf{q}) \sim \text{Re} \sum_{\delta} e^{i\mathbf{q} \cdot \delta}$, where δ runs over nearest and next-nearest neighbors. There must, in addition, be a short-range Coulomb pseudopotential, giving an interaction of unknown strength, but independent of *q*. The effective interaction is therefore

$$\chi(\mathbf{q}) = \chi_0 + \chi_1 \left[\cos(aq_x) + \cos\left(\frac{aq_x}{2} + \frac{\sqrt{3}aq_y}{2}\right) + \cos\left(\frac{aq_x}{2} - \frac{\sqrt{3}aq_y}{2}\right) \right] - \chi_2 \cos\left(\frac{cq_z}{2}\right) \left[\cos\left(\frac{\sqrt{3}aq_y}{3}\right) + 2 \cos\left(\frac{aq_x}{2}\right) \cos\left(\frac{\sqrt{3}aq_y}{6}\right) \right]. \tag{3}$$

The pairing potential V_q is given by

$$V_q = \begin{Bmatrix} 3 \\ -1 \end{Bmatrix} \frac{3}{4} I^2 \chi(\mathbf{q}), \tag{4}$$

where the upper (lower) factor corresponds to spin singlet (triplet) pairing and even (odd) parity. Since spin-orbit

coupling is not included, all components of the triplet gap have the same gap equation. Only the spatial representation of these components is determined. (The formalism of Ref. 9 is appropriate to a spin singlet pair wave function. It is then necessary to require that the spatial dependence of the gap be even under inversion. This constraint does not appear to have been consistently implemented.)

TABLE I. Basis functions for the various representations of D_6 . The interaction can be decomposed into sums of products of these functions.

| Representation | Function |
|----------------|--|
| A_{1g} | $\phi_k = \frac{1}{\sqrt{3}} \cos\left(\frac{ck_z}{2}\right) \left[\cos\left(\frac{\sqrt{3}ak_y}{3}\right) + \cos\left(\frac{ak_x + \sqrt{3}ak_y}{2} + \frac{\sqrt{3}ak_y}{6}\right) + \cos\left(\frac{ak_x - \sqrt{3}ak_y}{2} - \frac{\sqrt{3}ak_y}{6}\right) \right]$ |
| B_{1g} | $\psi_k = \frac{1}{\sqrt{3}} \sin\left(\frac{ck_z}{2}\right) \left[\sin\left(\frac{\sqrt{3}ak_y}{3}\right) + \sin\left(\frac{ak_x - \sqrt{3}ak_y}{2} - \frac{\sqrt{3}ak_y}{6}\right) - \sin\left(\frac{ak_x + \sqrt{3}ak_y}{2} + \frac{\sqrt{3}ak_y}{6}\right) \right]$ |
| E_{1g} | $\theta_k = \frac{1}{\sqrt{2}} \sin\left(\frac{ck_z}{2}\right) \left[\sin\left(\frac{ak_x + \sqrt{3}ak_y}{2} + \frac{\sqrt{3}ak_y}{6}\right) + \sin\left(\frac{ak_x - \sqrt{3}ak_y}{2} - \frac{\sqrt{3}ak_y}{6}\right) \right]$ |
| | $\xi_k = \frac{1}{\sqrt{6}} \sin\left(\frac{ck_z}{2}\right) \left[2 \sin\left(\frac{\sqrt{3}ak_y}{3}\right) + \sin\left(\frac{ak_x + \sqrt{3}ak_y}{2} + \frac{\sqrt{3}ak_y}{6}\right) - \sin\left(\frac{ak_x - \sqrt{3}ak_y}{2} - \frac{\sqrt{3}ak_y}{6}\right) \right]$ |
| E_{2g} | $\eta_k = \frac{1}{\sqrt{2}} \cos\left(\frac{ck_z}{2}\right) \left[\cos\left(\frac{ak_x + \sqrt{3}ak_y}{2} + \frac{\sqrt{3}ak_y}{6}\right) - \cos\left(\frac{ak_x - \sqrt{3}ak_y}{2} - \frac{\sqrt{3}ak_y}{6}\right) \right]$ |
| | $\zeta_k = \frac{1}{\sqrt{6}} \cos\left(\frac{ck_z}{2}\right) \left[2 \cos\left(\frac{\sqrt{3}ak_y}{3}\right) - \cos\left(\frac{ak_x + \sqrt{3}ak_y}{2} + \frac{\sqrt{3}ak_y}{6}\right) - \cos\left(\frac{ak_x - \sqrt{3}ak_y}{2} - \frac{\sqrt{3}ak_y}{6}\right) \right]$ |
| A_{2u} | $\phi'_k = \frac{1}{\sqrt{3}} \sin\left(\frac{ck_z}{2}\right) \left[\cos\left(\frac{\sqrt{3}ak_y}{3}\right) + \cos\left(\frac{ak_x + \sqrt{3}ak_y}{2} + \frac{\sqrt{3}ak_y}{6}\right) + \cos\left(\frac{ak_x - \sqrt{3}ak_y}{2} - \frac{\sqrt{3}ak_y}{6}\right) \right]$ |
| B_{2u} | $-\psi'_k = \frac{1}{\sqrt{3}} \cos\left(\frac{ck_z}{2}\right) \left[\sin\left(\frac{\sqrt{3}ak_y}{3}\right) + \sin\left(\frac{ak_x - \sqrt{3}ak_y}{2} - \frac{\sqrt{3}ak_y}{6}\right) - \sin\left(\frac{ak_x + \sqrt{3}ak_y}{2} + \frac{\sqrt{3}ak_y}{6}\right) \right]$ |
| E_{1u} | $\theta'_k = \frac{1}{\sqrt{2}} \cos\left(\frac{ck_z}{2}\right) \left[\sin\left(\frac{ak_x + \sqrt{3}ak_y}{2} + \frac{\sqrt{3}ak_y}{6}\right) + \sin\left(\frac{ak_x - \sqrt{3}ak_y}{2} - \frac{\sqrt{3}ak_y}{6}\right) \right]$ |
| | $\xi'_k = \frac{1}{\sqrt{6}} \cos\left(\frac{ck_z}{2}\right) \left[2 \sin\left(\frac{\sqrt{3}ak_y}{3}\right) - \sin\left(\frac{ak_x - \sqrt{3}ak_y}{2} - \frac{\sqrt{3}ak_y}{6}\right) + \sin\left(\frac{ak_x + \sqrt{3}ak_y}{2} + \frac{\sqrt{3}ak_y}{6}\right) \right]$ |
| E_{2u} | $\eta'_k = \frac{1}{\sqrt{2}} \sin\left(\frac{ck_z}{2}\right) \left[\cos\left(\frac{ak_x + \sqrt{3}ak_y}{2} + \frac{\sqrt{3}ak_y}{6}\right) - \cos\left(\frac{ak_x - \sqrt{3}ak_y}{2} - \frac{\sqrt{3}ak_y}{6}\right) \right]$ |
| | $\zeta'_k = \frac{1}{\sqrt{6}} \sin\left(\frac{ck_z}{2}\right) \left[2 \cos\left(\frac{\sqrt{3}ak_y}{3}\right) - \cos\left(\frac{ak_x + \sqrt{3}ak_y}{2} + \frac{\sqrt{3}ak_y}{6}\right) - \cos\left(\frac{ak_x - \sqrt{3}ak_y}{2} - \frac{\sqrt{3}ak_y}{6}\right) \right]$ |
| A_{1g} | $\phi''_k = \frac{1}{\sqrt{3}} \left[\cos(ak_x) + \cos\left(\frac{ak_x + \sqrt{3}ak_y}{2} + \frac{\sqrt{3}ak_y}{2}\right) + \cos\left(\frac{ak_x - \sqrt{3}ak_y}{2} - \frac{\sqrt{3}ak_y}{2}\right) \right]$ |
| B_{1u} | $\psi''_k = \frac{1}{\sqrt{3}} \left[\sin(ak_x) - \sin\left(\frac{ak_x + \sqrt{3}ak_y}{2} + \frac{\sqrt{3}ak_y}{2}\right) - \sin\left(\frac{ak_x - \sqrt{3}ak_y}{2} - \frac{\sqrt{3}ak_y}{2}\right) \right]$ |
| E_{1u} | $\theta''_k = \frac{1}{\sqrt{6}} \left[2 \sin(ak_x) + \sin\left(\frac{ak_x + \sqrt{3}ak_y}{2} + \frac{\sqrt{3}ak_y}{2}\right) + \sin\left(\frac{ak_x - \sqrt{3}ak_y}{2} - \frac{\sqrt{3}ak_y}{2}\right) \right]$ |
| | $\xi''_k = \frac{1}{\sqrt{2}} \left[\sin\left(\frac{ak_x + \sqrt{3}ak_y}{2} + \frac{\sqrt{3}ak_y}{2}\right) - \sin\left(\frac{ak_x - \sqrt{3}ak_y}{2} - \frac{\sqrt{3}ak_y}{2}\right) \right]$ |
| E_{2g} | $\eta''_k = \frac{1}{\sqrt{2}} \left[\cos\left(\frac{ak_x + \sqrt{3}ak_y}{2} + \frac{\sqrt{3}ak_y}{2}\right) - \cos\left(\frac{ak_x - \sqrt{3}ak_y}{2} - \frac{\sqrt{3}ak_y}{2}\right) \right]$ |
| | $\zeta''_k = \frac{1}{\sqrt{6}} \left[2 \cos(ak_x) - \cos\left(\frac{ak_x + \sqrt{3}ak_y}{2} + \frac{\sqrt{3}ak_y}{2}\right) - \cos\left(\frac{ak_x - \sqrt{3}ak_y}{2} - \frac{\sqrt{3}ak_y}{2}\right) \right]$ |

The interaction can be written in a separable form

$$V_q^{\text{even}} = \frac{1}{4} I^2 \chi_2 [\delta + (\phi_k'' \phi_{k'}'' + \eta_k'' \eta_{k'}'' + \zeta_k'' \zeta_{k'}'') - \phi_k \phi_{k'} - \psi_k \psi_{k'} - \theta_k \theta_{k'} - \xi_k \xi_{k'} - \eta_k \eta_{k'} - \zeta_k \zeta_{k'}], \quad (5)$$

$$V_q^{\text{odd}} = -\frac{3}{4} I^2 \chi_2 [\alpha (\psi_k' \psi_{k'}' + \theta_k' \theta_{k'}' + \xi_k' \xi_{k'}') - \phi_k' \phi_{k'}' - \psi_k' \psi_{k'}' - \theta_k' \theta_{k'}' - \zeta_k' \zeta_{k'}' - \eta_k' \eta_{k'}' - \xi_k' \xi_{k'}'],$$

$$\omega \Delta_k = - \sum_s k_s \frac{m_s^*}{m_e} \int \frac{d\phi d\theta}{4\pi} J_s \Delta_k \left\{ 3\delta + 3 \sum_{\substack{\Gamma\gamma \\ \text{even}}} [\alpha \Phi''(\Gamma, \gamma, k) \Phi''(\Gamma, \gamma, k') - \Phi(\Gamma, \gamma, k) \Phi(\Gamma, \gamma, k')] - \sum_{\substack{\Gamma\gamma \\ \text{odd}}} [\alpha \Phi''(\Gamma, \gamma, k) \Phi''(\Gamma, \gamma, k') - \Phi'(\Gamma, \gamma, k) \Phi'(\Gamma, \gamma, k')] \right\}. \quad (6)$$

T_c is an increasing function of ω ; therefore, the representation with highest eigenvalue is the stable one. The sum s is over the different pieces of the Fermi surface which have different quasiparticle masses m_s^* (Ref. 19) and different shapes,¹⁶⁻¹⁸ requiring different effective Fermi momenta k_s and Jacobian factors J_s . The $\Phi(\Gamma, \gamma, k)$ run over the basis functions, labeled by γ , of the different representations Γ . The number of primes on $\Phi(\Gamma, \gamma, k)$ matches the number of primes on the functions in Table I. UPt₃ has a center of inversion so that we can consider even- and odd-parity gaps separately.

To model the Fermi surface we have used the band calculations of Wang *et al.*¹⁷ and Oguchi *et al.*¹⁶ along with the deHaas-van Alphen measurements of Taillefer *et al.*¹⁹ The six different pieces of the Fermi surface are well approximated by ellipsoids. We include all of these and find that the most important contributions come from the prolate ellipsoids centered at Γ and the oblate ellipsoid centered at A .

For the even parity interaction we can write Δ_k as a linear combination of the even-parity functions listed in Table I. Substituting this into Eq. (7) gives a set of linear equations with coefficients determined by numerical wave-vector integration. These are then solved for the eigenvalues ω belonging to different representations. We find that the eigenvalues for the completely symmetric A_{1g} and the E_{1g} representations are much larger than the eigenvalues belonging to the other even representations. The A_{1g} and E_{1g} functions are labeled s and d , respectively, in Fig. 1.

A similar computation is carried out for the odd-parity interaction and we find that the eigenvalue for the E_{1u} representation is by far the largest among the odd-parity representations. This is the p state in Fig. 1.

From the results of our calculation we can draw a phase diagram for the adjustable parameters α and δ . Physically, α represents the strength of the ferromagnetic correlations relative to the antiferromagnetic part. δ represents the relative strength of the Coulomb pseudopotential. The phases are determined by which representation has the largest eigenvalue. From Fig. 1 it can be seen that antiferromagnetic spin fluctuations of the kind observed in UPt₃ do not necessarily give d -wave pairing. The isotropic repulsion represented by δ is important for allowing

where $\delta = \chi_0/\chi_2$, $\alpha = \chi_1/\chi_2$, and ϕ_k, ψ_k , etc. are functions listed in Table I that transform as single representations of D_6 . The notation used to label the representations follows Volovik and Gor'kov,²⁰ but the basis functions are different from their polynomial forms.

To determine the symmetry properties of the gap function we need the eigenvalues ω of the linearized gap equation

d -wave pairing as a possibility. With $\delta=0$, only s -wave or p -wave pairing is possible. δ does not contribute to ω for p - and d -wave states and the phase boundary is therefore vertical between these two.

We have done calculations of the eigenvalues varying the shapes and sizes of the Fermi-surface pieces. We find a rather strong dependence, indicating that this model may be able to account for the observed sensitivity of T_c to pressure,²¹ impurity concentration,²² etc. These results will be reported in a future publication.

Our calculations do confirm the theoretical expectation that antiferromagnetic correlations lead to d -wave pairing. They also show that care is needed in applying this reasoning to real systems where the interaction has several components and the Fermi surface is complicated. s - and p -wave states are not generally ruled out and indeed the s -wave state would be stable in the absence of short-range repulsions. The d -wave state most favorable by far for

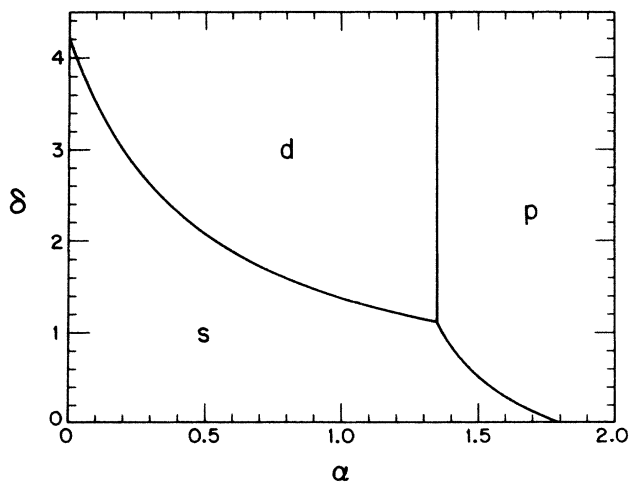


FIG. 1. Phase diagram for superconducting UPt₃, as a function of two undetermined interaction parameters α and δ . α represents the strength of in-plane ferromagnetic correlations. δ is the strength of a short-range isotropic repulsion. α and δ are dimensionless, being measured in units of the strength of the antiferromagnetic pairing potential.

UPt₃ is the E_{1g} state, which is twofold degenerate and has a line of nodes in the gap in the $k_z=0$ plane and a line of nodes in the plane $k_x=0$ or $k_y=0$. The most favorable p -wave state belongs to the E_{1u} representation. The p -wave functions in Table I have one line of nodes. This is due to our neglecting possible spin-orbit coupling which leads to such types of gap functions.²³ When this coupling is included, these lines of nodes become points, but we expect that the E_{1u} representation is still stable. We believe at the present time that realistic calculations of T_c are not possible owing to uncertainty in many parameters, most

notably the cutoff frequency, the renormalization of the Coulomb pseudopotential, and g factors arising from spin-orbit coupling which enter the interaction. On the other hand, one expects that whatever those parameters are, they enter in the same way for all of the different phases considered, and the conclusions concerning relative stability will be unaffected.

We would like to thank T. M. Rice and D. L. Huber for useful discussions.

¹For reviews, see C. M. Varma, *Comments Condens. Matter Phys.* **11**, 221 (1985); P. A. Lee, T. M. Rice, J. W. Serene, L. J. Sham, and J. W. Wilkins, *ibid.* **12**, 99 (1986); R. Joynt, *Phys. Scr.* **36**, 175 (1987); P. Fulde, J. Keller, and G. Zwicknagl (unpublished).

²C. M. Varma, *Phys. Rev. Lett.* **55**, 2723 (1985).

³P. W. Anderson, *Phys. Rev. B* **30**, 1549 (1984).

⁴O. T. Valls and Z. Tesanovic, *Phys. Rev. Lett.* **53**, 1497 (1984).

⁵K. Miyake, S. Schmitt-Rink, and C. M. Varma, *Phys. Rev. B* **34**, 6554 (1986).

⁶T. Matsuura, K. Miyake, H. Jichu, Y. Kuroda, and Y. Nagaoaka, *J. Magn. Magn. Mater.* **52**, 239 (1985).

⁷J. E. Hirsch, *Phys. Rev. Lett.* **54**, 1317 (1985).

⁸M. T. Beal-Monod, C. Bourbonnais, and V. J. Emery, *Phys. Rev. B* **34**, 7716 (1986).

⁹M. R. Norman, *Phys. Rev. Lett.* **59**, 232 (1987).

¹⁰A. Layzer and D. Fay, *Int. J. Magn.* **1**, 135 (1971).

¹¹P. W. Anderson and W. F. Brinkman, *Phys. Rev. Lett.* **30**, 1108 (1973).

¹²S. Nakajima, *Prog. Theor. Phys.* **50**, 1101 (1973).

¹³Y. Kuroda, *Prog. Theor. Phys.* **51**, 1269 (1974); **53**, 349 (1975).

¹⁴W. F. Brinkman, J. W. Serene, and P. W. Anderson, *Phys. Rev. A* **10**, 2386 (1974).

¹⁵G. Aeppli, A. Goldman, G. Shirane, E. Bucher, M.-Ch. Lux-Steiner, *Phys. Rev. Lett.* **58**, 808 (1987).

¹⁶T. Oguchi, A. J. Freeman, and G. W. Crabtree, *J. Magn. Magn. Mater.* **63-64**, 645 (1987).

¹⁷C. S. Wang, M. R. Norman, R. C. Albers, A. M. Boring, W. E. Pickett, H. Krakauer, and N. E. Christensen, *Phys. Rev. B* **35**, 7260 (1987).

¹⁸R. C. Albers and A. M. Boring, *Phys. Rev. B* **33**, 8116 (1986).

¹⁹L. Taillefer, R. Newbury, G. g. Lonzarich, Z. Fisk, and J. L. Smith, *J. Magn. Magn. Mater.* **63-64**, 372 (1987).

²⁰G. E. Volovik and L. P. Gor'kov, *Zh. Eksp. Teor. Fiz.* **88**, 1412 (1985) [*Sov. Phys. JETP* **61**, 843 (1985)].

²¹J. O. Willis, J. D. Thompson, Z. Fisk, A. de Visser, J. J. M. Franse, and A. Menovsky, *Phys. Rev. B* **31**, 1654 (1985).

²²B. Batlogg, D. J. Bishop, E. Bucher, B. Golding, Jr., A. P. Ramirez, Z. Fisk, J. L. Smith, and H. R. Ott, *J. Magn. Magn. Mater.* **63-64**, 441 (1987).

²³M. Ozaki, K. Machida, and T. Ohmi, *Prog. Theor. Phys.* **75**, 442 (1986).